

**EXPERIMENTAL TESTS ON DRIP SHIELD-WASTE  
PACKAGE MECHANICAL INTERACTION—  
PROGRESS REPORT**

*Prepared for*

**U.S. Nuclear Regulatory Commission  
Contract NRC-02-02-012**

*Prepared by*

**D. Pomerening<sup>1</sup>, L. Ibarra<sup>2</sup>, K. Hricisak<sup>1</sup>, T. Wilt<sup>2</sup>, K.T. Chiang<sup>2</sup>,  
R. Kazban<sup>2</sup>, and A. Chowdhury<sup>2</sup>**

**<sup>1</sup>Southwest Research Institute®**

**<sup>2</sup>Center for Nuclear Waste Regulatory Analyses  
San Antonio, Texas**

**September 2007**

## ABSTRACT

The drip shield and waste package are engineered barriers that the U.S. Department of Energy is considering for the potential geologic repository at Yucca Mountain, Nevada, where radioactive waste material would be encapsulated in waste packages and emplaced in tunnels. The drip shield protects the waste package from rockfall impacts and water intrusion as a result of seepage in the near-field environment. Independent structural analyses (Ibarra, et al., 2007a), however, indicate that the drip shield may not be able to withstand the expected static and dynamic loading conditions that might result from rockfall rubble accumulation. The potential drip shield structural instability may result in drip shield–waste package mechanical interaction that could lead to high localized plastic stresses in the waste package outer shell (Ibarra, et al., 2007b).

An experimental study is being performed to estimate the structural performance of the waste package outer shell when subjected to the loads transferred by a collapsed drip shield. The tests reproduce the numerical plane strain models evaluated by Ibarra, et al. (2007a). This progress report describes the experimental setup, plate deformation measurement techniques, and the interpretation of preliminary results. The experimental tests results are compared to those obtained from the numerical plane strain models. The tests also provide the performance of the Alloy 22 material for nonlinear states that cannot be predicted by only using finite element models with nondegrading constitutive relationships.

The report presents the results of the first experiment, which consists of a titanium “drip shield” plate contacting an Alloy 22 “waste package” plate at an angle of 45°. The test was performed at room temperature, and the loading was monotonically increased and discontinued after the maximum predefined threshold displacement was reached. The maximum recorded load was about one order of magnitude larger than the expected vertical static pressure and approximately two times the failure load initially predicted from the numerical models (Ibarra, et al., 2007b). The experimental and numerical load-displacement relationships, however, showed good agreement until the maximum load applied to the experimental test. This good correlation at high loads indicates that the local failure of some of the Alloy 22 elements contacting the tip of the titanium penetrator does not propagate. Also, failure appears to be self-arrested by the increase of the contact area as the titanium material penetrates the Alloy 22 plate.

## References

Ibarra, L., T. Wilt, G. Ofoegbu, and A. Chowdhury. “Structural Performance of Drip Shield Subjected to Static and Dynamic Loading.” San Antonio, Texas: Center for Nuclear Waste Regulatory Analyses. 2007a.

Ibarra, L., T. Wilt, G. Ofoegbu, R. Kazban, F. Ferrante, and A. Chowdhury. “Drip Shield–Waste Package Mechanical Interaction—Progress Report.” San Antonio, Texas: Center for Nuclear Waste Regulatory Analyses. 2007b.

# CONTENTS

Section	Page
ABSTRACT .....	ii
FIGURES .....	v
TABLES .....	vi
EXECUTIVE SUMMARY .....	vii
ACKNOWLEDGMENTS .....	x
1 INTRODUCTION.....	1-1
1.1 Background .....	1-1
1.2 Objectives and Scope.....	1-1
1.3 Outline of the Report .....	1-2
2 EXPERIMENTAL DESIGN AND SETUP .....	2-1
2.1 Description of Drip Shield–Waste Package Mechanical Interaction.....	2-1
2.1.1 Drip Shield and Waste Package Configuration.....	2-1
2.1.2 Drip Shield–Waste Package Mechanical Interaction .....	2-2
2.1.3 Waste Package Failure Mode.....	2-3
2.2 Experimental Setup .....	2-3
2.2.1 Test Components Geometry.....	2-4
2.2.1.1 Waste Package Representation .....	2-4
2.2.1.2 Drip Shield Bulkhead Representation.....	2-5
2.2.2 Testing Process .....	2-5
2.2.3 Output Data .....	2-7
2.2.3.1 Dynamic Structured Light Grating Projection Method.....	2-7
2.2.3.2 Coordinate Measuring Machine Method.....	2-7
2.3 Material Properties .....	2-9
3 EXPERIMENTAL RESULTS.....	3-1
3.1 Proof of Concept Experiment (DS–45–01).....	3-1
3.1.1 Loading.....	3-2
3.1.2 Load-Displacement History.....	3-2
3.1.3 Measurement of Plates Permanent Deformation.....	3-4
3.1.3.1 Plates Permanent Deformations According to the DSL Method.....	3-4
3.1.3.2 Permanent Plate Deformations According to the CMM Method .....	3-6
4 COMPARISON OF EXPERIMENTAL AND NUMERICAL PLANE STRAIN MODELS .....	4-1
4.1 Description of Two-Dimensional Plane Strain Model .....	4-1
4.2 Numerical Failure Mode for Plane Strain Models .....	4-1
4.3 Comparison of Experimental and Numerical Model Results .....	4-3

## CONTENTS (continued)

Section	Page
5 SUMMARY AND CONCLUSIONS.....	5-1
6 FUTURE WORK .....	6-1
7 REFERENCES.....	7-1

## FIGURES

Figure	Page
2-1	Isometric of Updated Drip Shield ..... 2-1
2-2	Configuration of 21-Pressurized Water Reactor Waste Package ..... 2-2
2-3	Representation of Drip Shield–Waste Package Mechanical Interaction ..... 2-3
2-4	Tinius-Olsen Super L Load Frame ..... 2-6
2-5	CMM Scan on Alloy 22 Plate Using a 60° Angle Touch Probe ..... 2-8
2-6	CMM Scan on Titanium Grade 5 Plate Using a 2-mm [0.079-in] Ruby Ball Touch Probe..... 2-8
2-7	Effect of Temperature on Materials Properties..... 2-11
3-1	Load Frame Configuration for DS–45–01 Test ..... 3-1
3-2	Test DS–45–01 at Maximum Applied Load..... 3-3
3-3	Permanent Deformation of Alloy 22 Plate in Test DS–45–01 ..... 3-3
3-4	Load-Displacement Curve for Test DS–45–01 ..... 3-4
3-5	DSL Scan of DS–45–01 Alloy 22 Plate ..... 3-5
3-6	DSL Scan of DS–45–01 Titanium Penetrator ..... 3-5
3-7	CMM Scan in X Director for DS–45–01 Alloy 22 Plate [1 in = 25.4 mm]..... 3-7
3-8	Detail of CMM Scan in X Direction for DS–45–01 Alloy 22 Plate..... 3-7
3-9	CMM Scan in X Direction of DS–45–01 Titanium Penetrator..... 3-8
4-1	Two-Dimensional Plane Strain Finite Element Model; Bulkhead Cross Section With Longitudinal Stiffener and Waste Package Outer Shell ..... 4-2
4-2	Plastic Distribution of Alloy 22 Plate at the Ultimate Tensile Strength ..... 4-4
4-3	Experimental (DS–45–01) and Numerical Load-Displacement Relationships ..... 4-4
4-4	Von Mises Stress Distribution of Alloy 22 Plate at the Maximum Experimental Load of DS–45–01 ..... 4-5
4-5	Plastic Strain Distribution of Alloy 22 Plate at the Maximum Experimental Load of DS–45–01 ..... 4-5
4-6	Plastic Strain Distribution of Titanium Plate at the Maximum Experimental Load of DS–45–01 ..... 4-6

## TABLES

Table		Page
2-1	Material Properties at 150 °C [302 °F].....	2-9
2-2	True Stresses and Strains for Titanium and Alloy 22 Materials at 150 °C [302 °F] .....	2-10
2-3	True Stresses and Strains for Titanium and Alloy 22 Materials at Room Temperature.....	2-10

## EXECUTIVE SUMMARY

The drip shield and waste package are part of several engineered barrier subsystems that the U.S. Department of Energy (DOE) is considering for the potential geologic repository at Yucca Mountain, Nevada, where the radioactive waste materials would be encapsulated in waste packages and emplaced in tunnels. The drip shields would protect the waste package from rockfall impacts and water intrusion as a result of seepage in the near-field environment. Independent structural analyses (Ibarra, et al., 2007a), however, indicate that the drip shield design DOE is currently considering (Bechtel SAIC Company, LLC, 2004) may not be able to withstand the expected static and dynamic loading conditions that might result from rockfall rubble accumulation. The potential drip shield structural instability may result in drip shield–waste package mechanical interaction that could lead to high localized plastic stresses in the waste package (Ibarra, et al., 2007b).

The waste package consists of an external cylinder (outer shell) made of Alloy 22 material and an internal cylinder made of stainless steel (inner vessel). Waste package failure is defined as breaching of the Alloy 22 waste package outer shell by the propagation of cracks through its thickness. The waste package inner vessel function is limited to providing structural support because cracks in the outer shell would permit the potential intrusion of water and cause the stainless steel inner vessel to deteriorate. Numerical plane strain finite element models were used to evaluate the potential for waste package failure due to mechanical interaction with a collapsed drip shield (Ibarra, et al., 2007b). Plane strain finite element models were created using simple geometric representations that permit the use of a highly refined mesh to capture the localized stresses and strains that occur due to the contact interaction. Also, three-dimensional finite element models were created to investigate the overall structural response of the drip shield–waste package interaction. The numerical failure limit state for the Alloy 22 plate is associated to the strain corresponding to the ultimate tensile strength (peak strength) of the material. Thus, this definition provides an estimate of the maximum vertical load that the waste package outer shell can withstand (i.e., vertical load carrying capacity) at the onset of failure.

To verify the structural performance obtained from the plane strain models, an experimental study was prepared to evaluate the capacity of Alloy 22 plates when subjected to loads transferred by Titanium Grade 5 [surrogate for Titanium 24 (Ankem and Wilt, 2006)] plates with different inclination angles (e.g., contact angles), temperature, and boundary conditions. This progress report describes the experimental setup used to reproduce the numerical plane strain models, as well as measurement techniques. The loads and deformations provided by the experimental tests can be compared to the numerical plane strain results in which loading was originally interrupted when the first Alloy 22 finite elements reached the ultimate tensile strength. More importantly, the tests provide insights into the performance of the Alloy 22 material for higher nonlinear states that could not be initially predicted by finite element models with nondegrading constitutive relationships.

The report presents the results of the first experiment, which consists of a titanium “drip shield” plate contacting an Alloy 22 “waste package” plate at an angle of 45°. The test was performed on as-received titanium and Alloy 22 material at room temperature under a displacement rate of 25.4 mm/min [0.01 in/min]. The threshold parameters for load application were the machine load capacity {1,779 kN [400 kips]} and a total deformation of 8.26 mm [0.325 in] between the titanium and Alloy 22 plates. The loading was monotonically increased and discontinued after

the maximum displacement of 8.265 mm [0.3254 in] was reached. The recorded load at this displacement was 1,690 kN [379.9 kips], equivalent to a load per unit length of 22,178 kN/m [1,520 kips/ft]. This load is about two times the load initially predicted by Ibarra, et al. (2007b) for the numerical failure limit state, but more than four times the load predicted by the numerical models when using the as-received material properties at room temperature. The difference in the numerical model results appears to be caused by the relatively large increase in the titanium material properties as the temperature decreases. Also, the experimental load is approximately one order of magnitude larger than the expected vertical static pressure at the crown of the drip shield (Ibarra, et al., 2007a).

The experimental and numerical load-displacement relationships, however, showed good agreement until the maximum load applied to the experimental test. The load-displacement curves correctly predicted the change of slope in the load-displacement curve at the loading level that causes some Alloy 22 elements to exceed the ultimate tensile strength. The good correlation between the titanium and Alloy 22 load-displacement curves after the numerical failure limit state is exceeded indicates that the local failure of the Alloy 22 elements contacting the tip of the titanium penetrator does not propagate rapidly. In addition, failure appears to be self-arrested by the increase of the contact area, as the titanium material penetrates the Alloy 22 plate.

The deformed elements confirmed that most of the deformation occurs in the Alloy 22 plate, which has less yield strength but much higher ductility properties than the Titanium Grade 5 components. The tip of the titanium penetrator yielded earlier in the process because of its sharp edge. However, once the tip was rounded, most of the deformation occurred in the Alloy 22 plate. Two techniques were evaluated to measure the permanent deformation field of the Alloy 22 and titanium plates. First, a three-dimensional surface measurement was performed using a dynamic structured light technique that characterizes the overall surface geometry. The second technique was the coordinate measuring machine method in which a stylus is moved across the surface of the material resulting in a line scan along the centerline of the plate. The results from both techniques were in good agreement with the deformation results obtained during the test. Also, there was no evidence of through-thickness cracks from the bottom of the groove to the bottom of the Alloy 22 plate.

A potential second stage of this experimental study would evaluate the effects of temperature, contact angle, and plate end conditions on the Alloy 22 plate when subjected to static loading. Initially, impact loading was expected to be included in this evaluation to simulate the dynamic loading that may be expected during a seismic event. This part of the project may not be necessary because of the better than expected performance of the Alloy 22 plate when subjected to static loading.

## References

Ankem, S. and T. Wilt. "A Literature Review of Low Temperature ( $<0.25T_m$ ) Creep Behavior of  $\alpha$ ,  $\alpha$ - $\beta$  and  $\beta$  Titanium Alloys." San Antonio, Texas: Center for Nuclear Waste Regulatory Analyses. 2006.

Bechtel SAIC Company, LLC. "Drip Shield Structural Response to Rockfall." 000-00C-SSE0-00300-000-00A. Las Vegas, Nevada: Bechtel SAIC Company, LLC. 2004.

Ibarra, L., T. Wilt, G. Ofoegbu, and A. Chowdhury. "Structural Performance of Drip Shield Subjected to Static and Dynamic Loading." San Antonio, Texas: Center for Nuclear Waste Regulatory Analyses. 2007a.

Ibarra, L., T. Wilt, G. Ofoegbu, R. Kazban, F. Ferrante, and A. Chowdhury. "Drip Shield–Waste Package Mechanical Interaction—Progress Report." San Antonio, Texas: Center for Nuclear Waste Regulatory Analyses. 2007b.

## ACKNOWLEDGMENTS

This report was prepared to document work performed by the Center for Nuclear Waste Regulatory Analyses (CNWRA) for the U.S. Nuclear Regulatory Commission (NRC) under Contract No. NRC-02-02-012. The activities reported here were performed on behalf of the NRC Office of Nuclear Material Safety and Safeguards, Division of High-Level Waste Repository Safety. This report is an independent product of CNWRA and does not necessarily reflect the views or regulatory position of NRC.

The authors thank B. Dasgupta for the technical review and Dr. D. Turner for the programmatic review of this report. The authors also express their appreciation to the NRC staff, including Dr. M. Nataraja, for their advice and counsel during planning and conducting this study. The authors also appreciate A. Ramos for providing word processing support in the preparation of the document and L. Mulverhill for editorial review.

## QUALITY OF DATA, ANALYSES, AND CODE DEVELOPMENT

**DATA:** All CNWRA-generated original data contained in this report meet quality assurance requirements described in the Geosciences and Engineering Division Quality Assurance Manual. Sources of other data should be consulted for determining the level of quality of those data. The work presented in this report is documented in Scientific Notebook 873.

**ANALYSES AND CODES:** CNWRA conducted finite element analyses using the commercial computer code ABAQUS/Standard Version 6.5 (ABAQUS, Inc., 2004), which is controlled under the software quality assurance procedure Technical Operating Procedure (TOP)-018, Development and Control of Scientific and Engineering Software. Spreadsheet calculations were accomplished using Microsoft® Excel® (Microsoft Corporation, 2002).

## References

ABAQUS, Inc. "ABAQUS User's Manual." Version 6.4. Providence, Rhode Island: ABAQUS, Inc. 2004.

Microsoft Corporation. "Microsoft® Excel® 2002.5P3." Redmond, Washington: Microsoft Corporation. 2002.

# 1 INTRODUCTION

## 1.1 Background

The U.S. Department of Energy (DOE) is studying the Yucca Mountain site in Nevada to determine whether it is suitable for building a geologic repository for the disposal of the spent nuclear waste. These radioactive materials would be encapsulated in waste packages and emplaced in tunnels excavated about 350 m [1,148 ft] below the ground surface. The drip shields would protect the waste packages from water intrusion due to seepage in the near-field environment and rockfall loading. However, an independent structural evaluation (Ibarra, et al., 2007a) of the drip shield design DOE is currently considering (Bechtel SAIC Company, LLC, 2004a) indicated that this barrier would exhibit structural instability for most loading configurations anticipated in a collapsed drift environment.

Because the loads transferred by the drip shield may lead to high localized stresses in the waste package, Ibarra, et al. (2007b) evaluated the potential breaching of the waste package using numerical plane strain finite element models. The models were created using simple geometric representations of the components to permit the use of a highly refined mesh. The numerical failure mode was associated to the strain corresponding to the ultimate tensile strength (peak strength) of the waste package outer shell material. Therefore, this definition provides an estimate of the maximum vertical load that the waste package outer shell can withstand (i.e., vertical load carrying capacity) at the onset of failure. This progress report presents the first results of an experimental study that reproduces the numerical plane strain models for different loading conditions

## 1.2 Objectives and Scope

An experimental study is performed to reproduce the structural performance of the waste package outer shell when subjected to concentrated stresses caused by a collapsed drip shield section. The curved shapes of the waste package and drip shield components are approximated using plates with flat surfaces under the assumption that waste package local deformation would not be greatly affected by the overall component configuration. The response of the Alloy 22 and titanium plates is compared to the waste package vertical load carrying capacity and components deformation obtained from numerical plane strain models (Ibarra, et al., 2007b) until the ultimate tensile strength of the Alloy 22 material is reached. Furthermore, the tests provide information about the performance of the Alloy 22 material for nonlinear states that cannot be predicted with finite element models using nondegrading constitutive relationships.

This progress report presents the experimental setup and quasi-static response of the waste package outer shell when load is transferred by a drip shield component at an inclined angle (contact angle) of 45°. The effects of temperature, contact angle, and plate end conditions may be evaluated at the second stage of the study, depending on the results of the first tests. Several phenomena that may affect the waste package mechanical performance, such as fabrication flaws, weld residual stresses, and hydrogen embrittlement, are not addressed in this study.

### **1.3 Outline of the Report**

This report is organized into six chapters. Chapter 2 describes the design of the experiments and physical setup for testing. The chapter describes the design of the tested components, the material mechanical properties, the load frame used for the tests, and the deformation measurement techniques. Chapter 3 presents the proof of concept experiment test performed at room temperature that consists of a titanium plate penetrating the Alloy 22 material at an angle of 45°. The load-deformation relationships obtained during testing and the scan tests of the permanent deformed plates are discussed. The comparison of the experimental results to the numerical plane strain models is provided in Chapter 4. Summary and conclusions are presented in Chapter 5, and potential future work is discussed in Chapter 6. The appendix provides the drawings used for the fabrication of the Alloy 22 and titanium plates.

## 2 EXPERIMENTAL DESIGN AND SETUP

### 2.1 Description of Drip Shield–Waste Package Mechanical Interaction

#### 2.1.1 Drip Shield and Waste Package Configuration

The drip shield section of the design the U.S. Department (DOE) is currently considering (Bechtel SAIC Company, LLC, 2004a) has a length of 5,805 mm [228.5 in], a cross-section width at the base of 2,533 mm [99.7 in], and a total height of 2,886 mm [113.6 in] (Figure 2-1). The drip shield consists of Titanium Grade 7 plates that are supported with frames made of Titanium Grade 24 equally spaced at 1,070 mm [42.1 in]. The drip shield base is made of Nickel Alloy N6022, commonly referred to as Alloy 22, and is the only drip shield structural component not made of titanium. The bulkhead refers to the reinforcing curved beam located at the drip shield crown, and the support beams are the columns of the drip shield frames spaced at 1,047 mm [41.2 in] (Bechtel SAIC Company, LLC, 2004a). The drip shield crown also includes three longitudinal stiffeners.

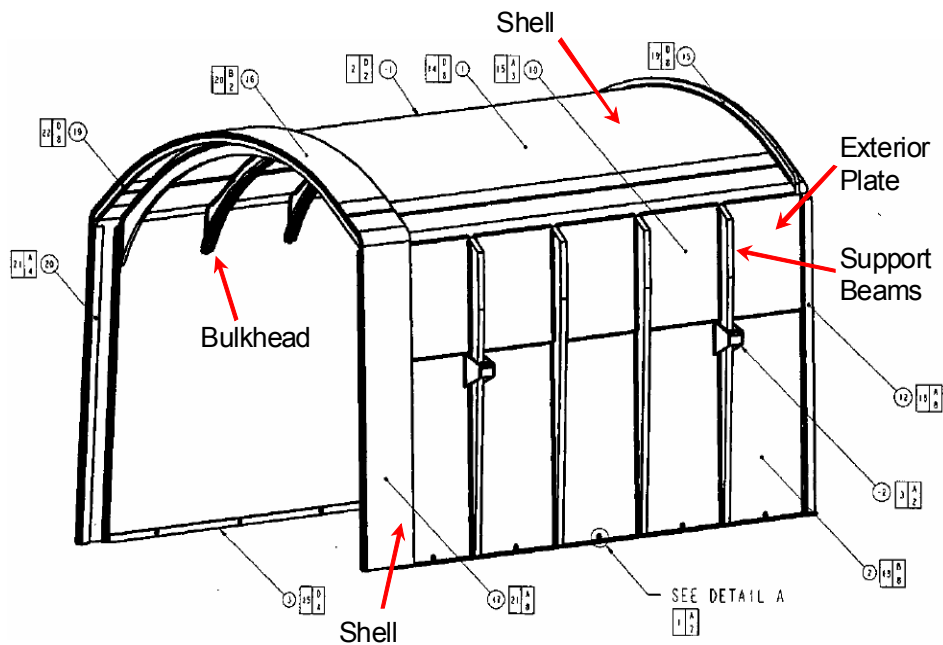


Figure 2-1. Isometric of Updated Drip Shield (Bechtel SAIC Company, LLC, 2004a)

The independent waste package evaluation is based on the configuration of the 21-Pressurized Water Reactor waste package (Figure 2-2) (Brown, 2004). The waste package is composed of two concentric cylinders separated by a gap of 4 mm [0.16 in]. The waste package outer shell is the external cylinder—a 20-mm [0.78-in]-thick plate made of Alloy 22. The internal cylinder is a 50-mm [1.97-in]-thick plate of 316 stainless steel referred to as the inner vessel. All waste packages rest on emplacement pallets that are uniformly sized.

## 2.1.2 Drip Shield–Waste Package Mechanical Interaction

Ibarra, et al. (2007a) predicted that for most loading configurations in a collapsed degraded environment, the drip shield design DOE is currently considering (Bechtel SAIC Company, LLC, 2004a) would collapse due to plastic buckling of the drip shield support beams (columns). The loads transferred by the collapsed drip shield to the waste package may lead to high localized stresses in the waste package outer shell. The magnitude of the stress concentrations is largely influenced by the angle between the drip shield component and the waste package outer shell (i.e., contact angle). A reduction in the contact area increases the potential for penetration of the drip shield component into the waste package or crack propagation in the waste package outer shell.

To evaluate the drip shield–waste package mechanical interaction, it was assumed that the bulkhead and the longitudinal stiffeners are the only drip shield components that may lead to waste package outer shell breaching (Figure 2-3). Because of the system geometry, the bulkhead is likely to have the initial contact and to cause the largest mechanical stresses on the waste package outer shell. The bulkhead leads to larger critical stresses because transfers more loads than the stiffeners.

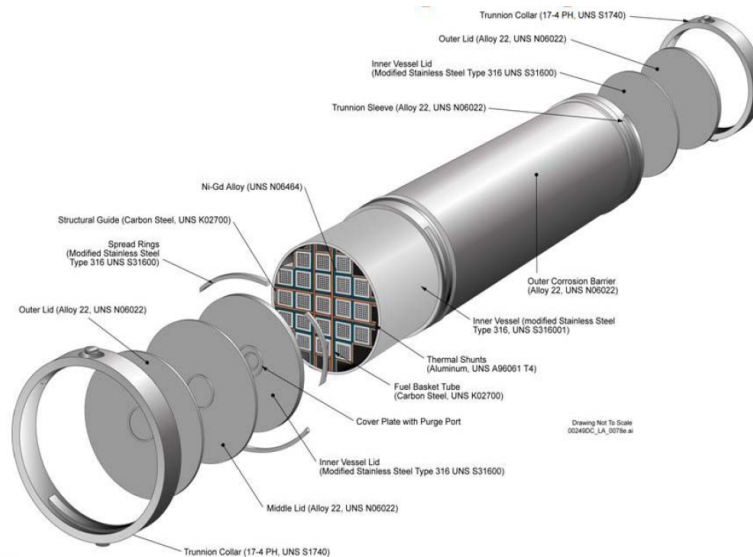


**Figure 2-2. Configuration of 21-Pressurized Water Reactor Waste Package (Brown, 2004)**

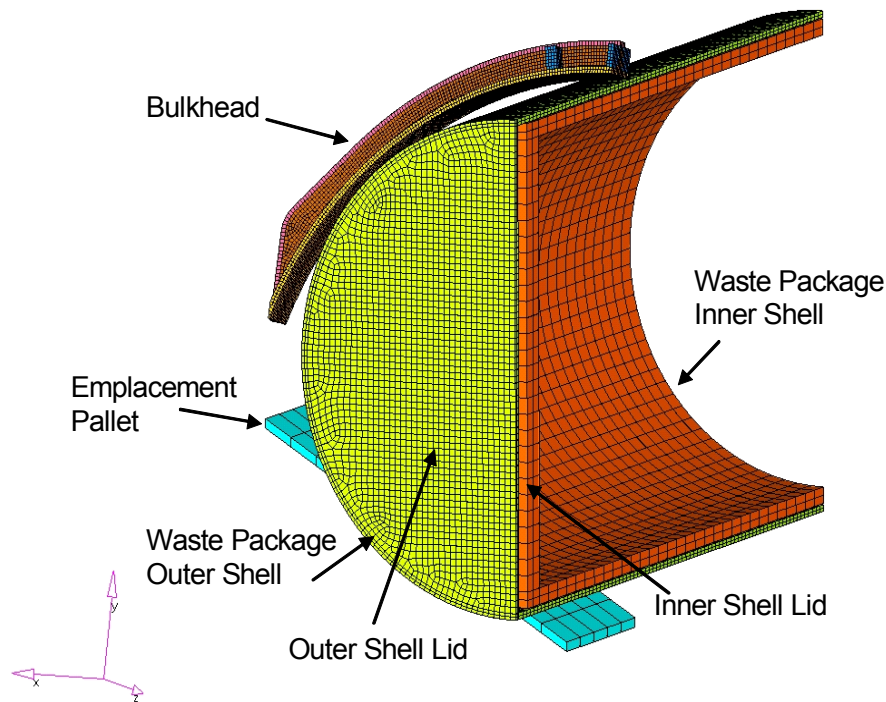


**Figure 2-3. Representation of Drip Shield–Waste Package Mechanical Interaction (Ibarra, et al., 2007b)**

### 2.1.3 Waste Package Failure Mode

Waste package failure refers to breaching of the Alloy 22 waste package outer shell, and it would be physically associated with cracks that propagate through the thickness of the outer shell. These cracks could permit the potential intrusion of water and cause the stainless steel inner vessel to deteriorate when exposed to Yucca Mountain chemical and environmental conditions. Thus in this evaluation, the waste package inner vessel function is limited to providing structural support, and breaching of the waste package outer shell represents waste package failure.

In Chapter 4, the experimental results will be compared to numerical plane strain finite element models. The numerical waste package outer shell failure limit state, however, was defined at the strain corresponding to the ultimate tensile strength (peak strength) of the material (Ibarra, et al., 2007b).

## 2.2 Experimental Setup

The curved shapes of the waste package and drip shield components are approximated using plates with flat surfaces under the assumption that local deformation would not be greatly affected by the overall component configuration. The response of the Alloy 22 and titanium plates is compared to the waste package vertical load carrying capacity and components

deformation obtained from numerical plane strain models (Ibarra, et al., 2007b) until the ultimate tensile strength of the Alloy 22 material is reached. Furthermore, the tests provide information about the performance of the Alloy 22 material for nonlinear states that cannot be predicted with finite element models using nondegrading models.

The geometry of the test components simulates the numerical plane strain models (Ibarra, et al., 2007b) used to evaluate the drip shield–waste package mechanical interaction. The sensitivity study performed on the numerical models indicated that the maximum load that the waste package can withstand (e.g., vertical load carrying capacity) is largely affected by the contact angle and the contact length. The experimental tests performed in this study are in accordance with the findings of the numerical models. The study evaluates the effect of the following parameters on the Alloy 22 plate capacity:

- Contact angle—The Alloy 22 plate will be loaded with titanium components with angles of 45°, 15°, and 5°. The 45° case results in a symmetrical loading condition and would be used to determine the influence of other factors on the test results. For this 45° case, the loading direction is expected to be vertical. For samples with contact angles of 15° and 5°, a lateral loading component would build up in the Alloy 22 plate.
- Boundary conditions—Although the analytical model is a two-dimensional plane strain model, the waste package Alloy 22 material would be partially constrained by the surrounding material in the cylindrical outer shell. Several tests would be performed to determine the influence of end constraints on the Alloy 22 waste package plate. If the load and deformation patterns are uniform over the majority of the test specimens, the assumption of two-dimensional plane strain is acceptable.
- Yucca Mountain Environmental Conditions—In the first stage, the as-received samples are tested at room temperature. Based on the results of the first experiments, some of the tests may be repeated at temperatures and chemical environmental conditions that better resemble the in-drift conditions.

## **2.2.1 Test Components Geometry**

For the experimental test, the curved shapes of the waste package and drip shield components are approximated using plates with flat surfaces under the assumption that waste package local deformation would not be greatly affected by the overall component configuration. Drawings of the test components are presented in the appendix and are described in the next sections.

### **2.2.1.1 Waste Package Representation**

In the experimental test, the waste package is represented with a flat Alloy 22 “waste package outer shell” plate and the “waste package” holder (appendix, p. 1 and 2). To simulate the “rigid” waste package inner vessel, the bottom surface of the Alloy 22 plate is supported directly on the load frame lower platen of the test machine. The waste package outer shell component is an Alloy 22 plate with a thickness of 19.1 mm [0.75 in], instead of the 20 mm [0.79 in] specified in Bechtel SAIC Company, LLC (2004b). The Alloy 22 plate dimensions are 76.2 × 152.4 × 19.1 mm [3.00 × 6.00 × 0.75 in], with a dimension tolerance of 0.254 mm [0.01 in]. The specimen width is limited by the capacity of the test machine. However, the selected width-to-thickness ratio has to be large enough to properly simulate the Alloy 22 plate deformation

response and to develop a quasi-two-dimensional response in the middle of the plate that is not affected by end conditions.

Restrained and unrestrained boundary conditions of the Alloy 22 plate can be considered in the study. For the unrestrained condition, the bottom surface of the Alloy 22 plate is supported directly on the load frame lower platen of the test machine. For the restrained condition, the Alloy 22 plate is located in the steel “waste package holder” (appendix, p. 2). This holder has a thickness of 12.7 mm [0.50 in] with tabs on the ends. The length of the plate and the tabs are designed to fit over the edges of the lower platen of the load frame. The Alloy 22 plate is accommodated at the 76.2 × 152.4 mm [3.00 × 6.00 in] central cutout. In the tests where full constraint of the Alloy 22 plate over its thickness plate is required, a modified “waste package holder” with additional plates welded at the ends of the cutout would be used as shown in the appendix, p. 3.

### **2.2.1.2 Drip Shield Bulkhead Representation**

The components that represent the drip shield in the experiment are the “titanium drip shield bulkhead penetrator,” the “drip shield” holder, and an upper support plate. Note that stainless steel support structures were designed to be significantly more rigid than the Alloy 22 and titanium plates to prevent additional spurious deformation. The drip shield bulkhead is modeled as a straight section of plate stock Titanium Grade 5 (surrogate for Titanium Grade 24<sup>1</sup>) that is machined to represent contact angles of 45°, 15°, and 5° (appendix, p. 4–6). By modifying the penetrator geometry, the primary load is vertical for all contact angles, which is consistent with the load frame capabilities. The titanium plate dimensions are 154.2 × 203.2 × 25.4 mm [6.00 × 8.00 × 1.00 in], and the 45°, 15°, and 5° angled sections add 19.1 mm [0.75 in] to its thickness. The length of the penetrator along the line of the loading is 203.2 mm [8.00 in], which is more than twice the width of the Alloy 22 plate. The contact angle between the titanium penetrator and the Alloy 22 plate is controlled by the tip of the wedge, which has a radius of 0.127 mm [0.005 in], in accordance with the numerical plane strain models. The total angle of the wedge for the contact angles is 90°.

The titanium penetrator is attached to a “drip shield holder” that has a thickness of 101.6 mm [4.00 in] and is sufficiently rigid to prevent additional deformation (appendix, p. 7). The drip shield holder is attached to a top plate measuring 457.2 × 457.2 × 38.1 mm [18.0 × 18.0 × 1.50 in] that is connected to the upper platen of the load frame (appendix, p. 8). The dimension tolerance for the “drip shield” components is also 0.254 mm [0.01 in].

## **2.2.2 Testing Process**

The load frame was selected based on the total force capacity, as well as the accuracy of the load and displacement instrumentation. The selected testing machine is a hydraulic actuated load frame (Tinius-Olsen Super L) that can apply a compressive load of 1,779 kN (400 kips) and displacements up to 228.6 mm [9.0 in] (Figure 2-4). To apply the loads, a Tinius-Olsen CMH

---

<sup>1</sup>Titanium Grade 5 is used as a surrogate material for Titanium Grade 24, which is not readily available. As discussed in Ankem and Wilt (2006), the material mechanical properties for both titanium alloys are very similar, although the chemical composition of Titanium Grade 24 includes a small amount of palladium to enhance corrosion resistance properties.



**Figure 2-4. Tinius-Olsen Super L Load Frame**

469 controllers are used, which can be programmed for up to eight combinations of rate-controlled load and displacement steps. The applied load and relative displacement between the upper and lower platens are measured by instrumentation built into the load frame.

The testing process is controlled by a process traveler, which identifies the following sequential steps necessary to accomplish the testing objectives:

- (1) Inspection and marking of the test items (Alloy 22 plate and titanium penetrator)
- (2) Verification of equipment calibration records
- (3) Facility configuration verification
- (4) Installation of test specimens
- (5) Identification of load parameters (load rate, maximum load, and maximum displacement)
- (6) Initial loading to 4.45 kN [1.0 kips]
- (7) Constant rate loading to either maximum load or maximum displacement
- (8) Unload test items
- (9) Removal of test items from load frame
- (10) Geometric measurement of test items
- (11) Repeat steps 4 to 10 for remaining load steps
- (12) Post-test load-displacement data reduction
- (13) Post-test geometric measurement data reduction

The results of these steps are documented on the process traveler and with photographs where applicable. During the test, load is monotonically increased to simulate a quasi-static load, and load-displacement time histories are monitored. At the conclusion of each load cycle, the test item geometry is characterized, particularly the plastic deformation along the contact line.

### **2.2.3 Output Data**

The testing output information includes the overall load-displacement response of the test assembly and the local deformation of the Alloy 22 and titanium plates. The applied load and relative displacement between the upper and lower platens are measured by instrumentation built into the load frame. Based on calibration records, the maximum error in the applied load is 0.56 percent with a resolution of 43.6 N [9.8 lb], and the maximum displacement error is 0.5 percent with a fixed error of  $\pm 5.0 \mu\text{m}$  [ $\pm 0.0002$  in]. Two techniques are initially used to measure the deformation field of the Alloy 22 and titanium plates. First, a three-dimensional surface measurement is performed using a Dynamic Structured Light (DSL)<sup>2</sup> technique that characterizes the overall surface geometry. The second technique is the Coordinate Measuring Machine (CMM)<sup>3</sup> method, in which a stylus is moved across the surface of the material resulting in a line scan along the centerline of the plate.

#### **2.2.3.1 Dynamic Structured Light Grating Projection Method**

The DSL three-dimensional (patent pending) measurement process is based on quadric surfaces defined by a projected and rotating light grid pattern (Franke, et al., 2004). The X, Y, and Z coordinates of a point on a measured surface are calculated from the intersection of a pixel ray from the camera and a quadric surface. The DSL three-dimensional system has been used to measure small parts {approximately  $50.8 \times 50.8$  mm [ $2.0 \times 2.0$  in]} with an accuracy of 0.102 mm [0.004 in].

#### **2.2.3.2 Coordinate Measuring Machine Method**

A CMM machine generates three-dimensional points from a surface, usually in terms of X, Y, and Z coordinates. The Brown & Sharpe Global Image 09-15-08 used in the program is used in an automatic scanning mode. The scanning probe is moved over the part surface and points are generated. For scanning the Alloy 22 plate, a 60°-angle touch probe tip is used (Figure 2-5). This probe has a sharp point that penetrates into the full depth of the groove. The titanium penetrator is scanned with a 2-mm [0.078-in] ruby ball touch probe (Figure 2-6). The ball allows the tip to ride over the surface of the penetrator to accurately measure the peak. For both plates, scan points are obtained every 0.318 mm [0.0125 in] perpendicular to the contact line (X-axis) and along the contact line (Y-axis).

---

<sup>2</sup>Dynamic Structured Light is referenced frequently throughout this report. The acronym DSL will be used.

<sup>3</sup>Coordinate Measuring Machine is referenced frequently throughout this report. The acronym CMM will be used.